ANTIOXIDANTS & REDOX SIGNALING
Volume 8, Numbers 9 & 10, 2006

Forum Original Research Communication

NAD(P)H Oxidase Activity of Nox4 in Chondrocytes Is Both Inducible and Involved in Collagenase Expression

LAURENT GRANGE,[1,2]* MINH VU CHUONG NGUYEN,[1]* BERNARD LARDY,[1]
MADIHA DEROUAZI,[1] YANNICK CAMPION,[1] CANDICE TROCME,[1]
MARIE–HELENE PACLET,[1] PHILIPPE GAUDIN,[1,2] and FRANCOISE MOREL[1]

ABSTRACT

Reactive oxygen species (ROS) are regulators of redox-sensitive cell signaling pathways. In osteoarthritis, human interleukin-1β is implicated in cartilage destruction through an ROS-dependent matrix metalloproteinase production. To determine the molecular source of ROS production in the human IL-1β (hIL-1β)-sensitive chondrocyte immortalized cell line C-20/A4, transfected cells were constructed that overexpress NAD(P)H oxidases. First, RT–PCR analysis showed that the C-20/A4 cell line expressed Nox2, Nox4, p22*phox*, and p67*phox*, but not p47*phox*. It was found that ROS production by C-20/A4 chondrocytes does not depend on PMA and ionomycin activation. This indicates that Nox2 was not involved in the production of ROS. In C-20/A4 cells that overexpress Nox4, hIL-1β stimulated ROS production three times more than the normal production of C-20/A4 cells. Moreover, there was a fourfold increase in the production of collagenase (MMP-1) by chondrocytes that overexpress Nox4. Interestingly, MMP-1 production in cells that overexpress Nox2 was not sensitive to hIL-1β. These data suggest that under hIL-1β stimulation, C-20/A4 chondrocytes produce MMP-1 through a Nox4-mediated, ROS-dependent pathway. *Antioxid. Redox Signal.* 8, 1485–1496.

INTRODUCTION

In recent years it has become evident that reactive oxygen species (ROS), such as superoxide and hydrogen peroxide, act as important regulators of redox-sensitive cell signaling pathways. ROS are involved in diverse cellular processes, such as host defense, oxygen sensing, proliferation, apoptosis, and response to mechanical strain. However, in a pathological sense, overproduction of ROS has been associated with inflammation, vascular atherosclerosis, diabetes, hypertension, tumorigenesis, and osteoarthritis (OA) (26). Osteoarthritis represents one of the most frequent musculoskeletal diseases, affecting over 60% of the elderly population. The pathogenesis of primary osteoarthritis involves an intrinsic and progressive erosion of articular cartilage, leading to incapacity of movement and chronic pain. An imbalance between anabolic and catabolic pathways by chondrocytes occurs in OA (2). These catabolic pathways are characterized by an excessive production of proteolytic enzymes, the matrix metalloproteinases (MMPs), which are directly involved in cartilage resorption.

Articular chondrocytes actively produce ROS, released in response to interleukin-1β (26–42). It has been suggested that ROS act as secondary messengers in bovine chondrocytes and are involved in mitogen-activated protein kinase (MAPK) stimulation, and c-jun and NF-kappaB activation required for transcription of cytokine-induced MMP-1 (collagenase-1) and MMP-13 (collagenase-3) metalloproteinases (22, 25, 28, 48).

Recent studies indicate that NAD(P)H oxidases play a major role in ROS production in many nonphagocytic cells (14, 15). It has been proposed that NAD(P)H oxidase Nox2 (gp91*phox*) could produce superoxide anions in the immortalized chondrocyte cell line C-20/A4, similar to those found in phagocyte cells (15, 30, 31). However, the involvement of Nox2 in superoxide production in osteoarthritis has not been proven. In porcine chondrocytes, no production of ROS was seen after addition of phorbol ester (PMA), a Nox2 activator (15). Indeed, p47phox and gp91*phox*-deficient mice have the same tissue damage as wild type mice in experimental arthritis models (another joint disease) (45). Recent efforts to identify oxidases responsible for ROS generation in nonphagocytic cells led to the discovery of

Center for Biomedical EPR Spectroscopy and Imaging, and Comprehensive Wound Care Center, Davis Heart and Lung Research Institute, The Ohio State University, Columbus, Ohio.

gp91^{phox} isoforms. To date, the Nox family consists of five members, all of which are structurally similar to the Nox2 protein (20). One member of this family, Nox4, is the major source of ROS in kidneys (9, 11) and is also abundant in the vascular system and in many others tissues (19). In osteoclast cells, Nox4 has been identified and shown to produce superoxide that directly contributes to bone resorption (49). Strong evidence indicates that superoxide production in chondrocytes could be responsible for the overexpression of metalloproteinases.

To address these questions, we studied the effect of the expression of the Nox family and its partners in chondrocyte immortalized cell lines. We focused our study on Nox4 and Nox2, and used the C-20/A4 chondrocyte cell line, which provides a stable expression of both protein types to compare their roles under cytokinic stress and their impact on MMP-1 expression. In this study, we report that Nox4 is the main NAD(P)H oxidase involved in ROS production under human interleukin-1beta (hIL-1β) stimulation in the C-20/A4 chondrocyte cell line, and that ROS are directly related to MMP-1 production.

MATERIALS AND METHODS

Materials and cells

Human chondrocyte cell lines immortalized by SV40, C-20/A4, T/C-28a2, or C-28/I2, are a gift from M.B. Goldring (Harvard Institutes of Medicine, Boston, MA). Monoclonal antibodies anti-p22^{phox} 44.1 and monoclonal antibodies anti-Nox2 (54.1 & NL7) were from A.J. Jesaïtis (Montana State University, Bozeman, MT) monoclonal antibodies anti-Nox2 7D5 were purchased at MBL Medical & Biological Laboratories Co., Ltd (NaKa-ku Nagoya, Japan) and monoclonal antibodies antihistidine from Qiagen (Courtaboeuf, France). Irrelevant monoclonal IgG1 was obtained from Immunotech (Marseille, France) and phycoerythrine-conjugated secondary antibodies from Dianova (Hamburg, Germany). Penicillin, streptomycin, L-glutamine, Dulbecco's modified Eagle's medium (DMEM), fetal bovine serum (FBS), trypsin, EBSS, geneticin, and TRIzol® were obtained from Invitrogen (Cergy Pontoise, France). Human IL-1beta (hIL-1β) and LightCycler FastStart DNA Master plus SYBR Green I kit were purchased from Roche Applied Science (Meylan, France), blasticidin from Funakoshi Co (Japan), and AMV reverse transcriptase from QBiogene (Illkirch, France). ProMMP-1 ELISA kits were obtained from R&D Systems (Lille, France) and Effectene Transfection reagent from Qiagen. Luminol, ionomycin, phorbol 12-myristate 13-acetate (PMA), horseradish peroxidase, and dihydroethidium were from Sigma (Saint Quentin Fallavier, France).

Chondrocyte cell line culture

C-20/A4, T/C-28a2, and C-28/I2 chondrocyte cell lines were maintained in DMEM supplemented with 10% (v/v) FBS, 100 units/ml penicillin, 100 µg/ml streptomycin, 2 m*M* L-glutamine at 37°C in a humidified 5% CO_2 atmosphere. Blasticidin, 10 µg/ml, was added to the culture medium of cells transfected with the mammalian expression plasmid pEF_b (Invitrogen, Cergy Pontoise, France) and 1 µg/ml geneticin was added to the culture medium of Nox2 transfected cells. All experiments were performed within cell passages 3 to 10 at 60–90% confluency.

Generation of plasmid constructs for the expression of Nox4 isoforms and Nox2

Human Nox4 and Nox2 were cloned: two Nox4 cDNA ESTs were characterized by PCR using UNI-ZAP human kidney lambda cDNA library (Stratagene, La Jolla, CA) as a template. Nox4A corresponds to the full-length Nox4 usually described in Genbank No.AF254621, and Nox4B is an exon 14 spliced isoform (Genbank No.AJ704726). N-terminal V5-His-tagged Nox4A and Nox4B were produced with the forward primer Nox4 F4′′′ (5′-GTTT**GGTACC**ATGGCTGTGTC-CTGGAGG-3′) including a Kpn I site (shown in **bold type**) and the reverse primer Nox4 R4' (5′-GTTT**ACTAGTG**CT-GAAAGACTCTTTATTGTATTC-3′) comprising a Spe I restriction site (shown in **bold type**) instead of the stop codon. Both purified PCR products were subcloned into the pCR Blunt II-TOPO vector according to the manufacturing protocol (Zero Blunt TOPO PCR cloning kit, Invitrogen). pCR-BluntII-TOPO plasmid containing Nox4A or Nox4B was digested by Kpn I and Spe I, and the insert was ligated into a linearized pEF6V5/HisB vector (Invitrogen). Dominant-negative pCDNA 3.1 Nox4 ΔFAD/NADPH plasmid was constructed using the forward primer Nox4 F4 and the reverse primer Nox4 R4′′ (5′-GTTT**GCGGCCGC**TCAAATGATG-GTGACTGGCTTATTGC-3′) containing a Not I restriction site (shown in **bold type**). This purified PCR product was digested by Kpn I and Not I and ligated into linearizd pCDNA 3.1 V5/HisB vector (Invitrogen). The construction that expressed Nox2 in pEF-PGK neo plasmid was obtained from Stasia *et al.* (39). All inserts were verified by sequencing (Genome Express, Grenoble, France) on an Abi Prism automatic sequencer (Perkin Elmer, France Office).

Transfection of mammalian expression plasmids

Stable transfection. C-20/A4 chondrocyte cells were trypsinized and counted. 4×10^5 C-20A/4 cells were seeded in 6-well plates and allowed to grow for 24 h to reach a 60% confluency in a 2 ml DMEM culture medium. Cells were transfected with 0.4 µg of pEF6V5HisB vectors, which encoded the Nox4A-V5/His, or the Nox4B-V5/His, or with pEF-PGK neo, which encoded Nox2 according to the manufacturing protocol (Effectene Transfection reagent, Quiagen, Courtaboeuf, France). After 24 h, stable transfected cells were selected with either 10 µg/ml blasticidin for Nox4A-V5/His, Nox4B-V5/His, and luciferase, or 1 mg/ml geneticin for Nox2 for 3 weeks (37).

Transient transfection. C-20/A4 chondrocyte cells were seeded in a 25 cm^2 flask to obtain 50% confluency on the day of transfection. Five µg of plasmid of pCDNA 3.1 V5/His empty vector (Invitrogen) or pCDNA 3.1 Nox4 ΔFAD/NADPH were diluted in 200 µl of CaCl2 (250 m*M*) buffer and 200 µl of HEPES-phosphate buffer (140 m*M* NaCl, 50 m*M* HEPES, 1.4 m*M* NaH2PO4, pH 7.05) was added. After 60 sec of incubation at room temperature, the transfection solution was added to cells immersed in 1.8 ml of complete DMEM culture medium. Four hours after transfection, the medium was replaced. Forty-eight hours after transfection, the quantity of MMP-1 was measured as described below.

RNA and RT–PCR

Chondrocytes were harvested and resuspended in TRIzol® at approximately 10^8 cells/ml, as described in the manufacturer's instructions. RNA concentrations were determined spectroscopically at 260 nm. Reverse transcription reactions were performed from 5 µg of RNA with 20 U of AMV reverse transcriptase, as described in Trocme *et al.* (44). All PCRs were processed during 35 cycles from 2.5 µl cDNA with 2.5 U of *Taq* polymerase and primer sets spanning intron/exon boundaries to avoid genomic DNA amplification (Table 1). Two primer sets were used to characterize Nox4, the first—F4/R4—amplifying a 500 bp sequence in the 5' part of the transcript (40) and the second—F4′/R4′—differentiating the two Nox4 isoforms at 1317 bp for Nox4A and 1197 bp for Nox4B. cDNA integrity and quantity were checked by amplification of a housekeeping gene G3PDH using commercial primers (BD Bioscience, Le Pont de Claix, France).

Quantitative real-time RT–PCR analysis

Total RNA was extracted from C-20/A4 cells using Trizol reagent (Invitrogen), according to the manufacturer's instructions. Two µg of RNA were converted to cDNA by reverse transcription with 40 U of AMV reverse transcriptase (Roche). Expression levels of human Nox-4 and housekeeping G3PDH mRNAs were determined using the specific primers as follows: forward Nox-4 F4′′′ (5′-CTGAATGCAGCAAGATACCGAGAT-3′) and reverse Nox-4 R4′′′ (5′-CTGGCTTATTGCTCCGGA-3′), and forward G3PDH F9 (5′-GTGGTGGACCTGACCTGC-3′) and reverse G3PDH R9 (5′-CCCTGTTGCTGTAGCCAAATTCG-3′). Real-time quantitative Nox4 and G3PDH PCRs of each reverse-transcribed cDNA sample were made on the Light Cycler 1.5 apparatus using the LightCycler FastStart DNA Master plus SYBR Green I kit (Roche). The incubation conditions were as follows: 95°C for 10 min, followed by 45 cycles of denaturation at 95°C for 15 sec, annealing at 66°C for 10 sec for Nox4 or G3PDH, and extension at 72°C for 21 sec for Nox4, or 10 sec for G3PDH. PCRs of each sample were done in duplicate. Nox4 mRNA expression was quantified by relating the PCR cycle obtained from samples to a standard curve and was then normalized to the G3PDH mRNA expression level. Product specificity was confirmed for each fragment by a melting curve analysis and gel electrophoresis.

FACS analysis

Protein expression of $p22^{phox}$, Nox2 ($gp91^{phox}$), Nox4A-V5/His, and Nox4B-V5/His in the human C-20/A4 chondrocyte cell line was assessed by flow cytometry analysis, according to Stasia *et al.* (38) and Paclet *et al.* (34), and was modified as follows: 5×10^5 cells were fixed with 1% (w/v) paraformaldehyde for 15 min at 0°C and labeled with antibodies immediately or after membrane permeabilization by saponin 0.01% (w/v) for 10 min at 0°C. Nox2 expression was evaluated with monoclonal antibodies 7D5 (5 µg/5×10^5cells), NL7 (5 µg/5×10^5cells), 54.1 (5 µg/5×10^5cells) (32), and $p22^{phox}$ expression was characterized with monoclonal antibodies 44.1 (5 µg/5×10^5cells) (6).

Nox4A-V5/His and Nox4B-V5/His expression were assessed by two polyclonal antibodies, the former raised against the polyhistidine tail (5 µg/5×10^5cells), and the latter against the Nox4 peptide ^{88}KVPSRRTRRLLDKSR^{102}, synthesized by Neosystem (Strasbourg, France) (5 µg/5×10^5cells) (35).

TABLE 1. PRIMER SEQUENCES USED IN THIS STUDY

Name	Primers (5'... 3')
	Nox1
F1	GTACAAATTCCAGTGTGCAGACCAC
R1	AGACTGGAATATCGGTGACAGCA
	Nox2
F2	ATAAGCAGGAGTTTCAAGAT
R2	GTTTTCTAGACTGAAGTTTTCCTTGTTGAAAATGAAATG
	Nox3
F3	ATGAACACCTCTGGGGTCAGCTGA
R3	GGATCGGAGTCACTCCCTTCGCTG
	Nox4
F4	CAGCAAGATACCGAGATG
R4	CTGGCTTATTGCTCCGGA
F4'	CTGAATGCAGCAAGATACCGAGATG
R4'	GTTTACTAGTGCTGAAAGACTCTTTATTGTATTC
R4"	GTTTGCGGCCGCTCAAATGATGGTGACTGGCTTATTGC
F4"'	CTGAATGCAGCAAGATACCGAGAT
R4"'	CTGGCTTATTGCTCCGGA
	Nox5
F5	ATCAAGCGGCCCCCTTTTTTTCAC
R5	CTCATTGTCACACTCCTCGAC
	$p22^{phox}$
F6	CAGTGTCCCAGCCGGGTTCGTGTC
R6	ATTGCAGGTGGGTGCACCTGGTGGGAG
	$p67^{phox}$
F7	TGTCTTTGTCTTGAAGAAGGGC
R7	GACTTCTCTCCGAGTGCTTTC
	$p47^{phox}$
F8	GAGCACTGGGGGCCACCCAGTC
R8	GTTTTATGGAACTCGTAGATCTCCG
	$p40^{phox}$
F9	TGGCAGCTCCGAGAGCAGAG
R9	GGCATCGTGTTGTAGACCCTG
	G3PDH
F10	GTGGTGGACCTGACCTGC
R10	CCCTGTTGCTGTAGCCAAATTCG

Monoclonal IgG1 (5 µg/5×10^5cells) was used as a control. The antibody-labeled cells were stained with phycoerythrine-conjugated secondary antibodies (dilution 1:200), and the fluorescence emission was measured at 578 nm after excitation at 488 nm on a FACS Calibur apparatus (BD Bioscience). All experiments were performed in triplicate.

Cytochrome b spectroscopy

The cytochrome *b* absorption spectra were performed with the C-20/A4 chondrocyte cell line WT, or transfected with the Nox4 gene resuspended in a PBS buffer containing 1% of triton ×100. They were recorded at room temperature with a DU 640 spectrophotometer (Beckman Coulter, Roissy, France). Reduction was achieved in the cuvette by addition of

a few grains of sodium dithionite, and reduced minus oxidized difference spectra were recorded. The amount of reduced cytochrome b_{558} was determined by absorbancy at 426 nm using an $\epsilon_{426\ nm}$ value of 106 mM^{-1}cm^{-1}, or at 558 nm ($\epsilon_{558\ nm}$ = 21.3 mM^{-1}cm^{-1}). A positive control was performed on cytochrome b_{558} purified from human neutrophils (33).

Measurement of NADPH oxidase activity in intact cells by luminescence assay

Hydrogen peroxide production was measured as described in Bionda *et al.* (3). Briefly, cells were washed twice with PBS, detached with trypsin and collected by centrifuge. The viability of the suspended cells was over 90%, as determined by the trypan blue exclusion method. In a 96-well plate, 5×10^5 live chondrocytes per well were resuspended in 250 µl of PBS containing 0.9 m*M* $CaCl_2$, 0.5 m*M* $MgCl_2$, 16 m*M* glucose, 16 µ*M* luminol, and 8 units/ml horseradish peroxidase. In some experiments, a final concentration of 80 ng/ml phorbol myristate acetate (PMA) or 2.5 µ*M* ionomycin was added to initiate the reaction. Relative luminescence unit (RLU) counts were recorded every 30 sec for a total of 90 min at 37°C, using a Luminoscan® luminometer (Labsystems, Helsinki, Finland).

Measurement of superoxide production in intact cells by fluorescence microscopy

Cell cultures were made in a 6-well plate until 80% confluency. Cells were rinsed twice with EBSS and incubated in 1 ml of the complete culture medium (DMEM-10% FBS) containing 5 µ*M* final dihydroethidium (DHE) with or without hIL-1β (500 pg/ml) for 20 min at 37°C in a 5% CO_2 atmosphere protected from light. In some experiments, *N*-acetylcysteine 30 n*M* (NAC) final was added. Fluorescence was recorded with a Nikon digital sight DS-1QM (Nikon, Rollay, France), mounted on a Nikon eclipse TE2000-E fluorescence microscope (Nikon). Dihydroethidium fluorescence was analyzed using a filter with an excitation wavelength of 488 nm and an emission wavelength of 580 nm. Images were acquired 20 min after DHE addition using identical exposure times, and analyzed with the Lucia software (Lucia Imaging systems, Laboratory Imaging Ltd, Prague, Czech Republic). Relative superoxide levels between cells were quantified by determining the integral gray values using Lucia Imaging systems. The integral gray value is defined as the sum of intensity in every pixel of the object. A minimum of 50 cells were analyzed per experiment. Results were expressed in arbitrary units.

MMP-1 assays

Cells cultured at 90% confluency in a 75 cm^2 flask were washed three times in EBSS and incubated for 23 h in 15 ml of FBS-free DMEM with or without 500 pg/ml hIL-1β, in the presence or not of 5 m*M* Tiron. For inhibition experiments using the dominant-negative construct pCDNA Nox4 deltaFAD/NADPH, cells cultured at 50% confluency in a 25 cm^2 flask for 48 h after transient transfection were washed three times in EBSS and incubated for 23 h in 2 ml of FBS-free DMEM, with or without 500 pg/ml hIL-1β. At the end of the incubation, proMMP-1 (the precursory form of MMP-1) concentration was measured in the supernatant culture by a commercial ELISA assay. The detection limit was 0.021 ng/ml. Results are expressed as ng proMMP-1/g of supernatant protein, measured by the Bradford technique (4).

Statistical methods

The variations are expressed as mean ± S.E.; p values were calculated by Student's paired t test.

RESULTS

Superoxide production is involved in hIL-1β stimulation of MMP-1 expression

Treatment of the C-20/A4 chondrocyte cell line with hIL-1β for 23 h significantly increased the secretion of collagenase MMP-1 in the culture medium from 136.28 ng/g of supernatant protein ± 63.54 to 913.36 ng/g of supernatant protein ± 64.54, suggesting an effect of hIL-1β on metalloproteinase expression (Fig. 1). Since it has been proposed that ROS may act as secondary messengers in cytokine signaling (23, 27), antioxidants that can inactivate ROS would be expected to prevent MMP-1 induction by hIL-1β. We therefore examined whether Tiron, a superoxide scavenger, can inhibit hIL-1β-induced MMP-1 expression. Indeed, the release of MMP-1 was considerably decreased by Tiron to 13.75 times in cells activated by hIL-1β and even by 6.97 times in control cells. We verified that neither Tiron nor hIL-1β affected cell integrity through the LDH measurement in the cell culture medium at the end of each experiment (data not shown).

Expression of Nox and partners in chondrocyte cell lines

In most cell types, the Nox family is the main system involved in superoxide production. There are five human NADPH oxidases, namely Nox1 to Nox5. To determine if C-20/A4, C-28/I2, and T/C-28a2 chondrocyte cell lines express genes encoding components of NADPH oxidases, the presence of the relevant mRNA was estimated by RT–PCR. cDNA integrity was checked simultaneously by amplification of the housekeeping gene G3PDH (results not shown). The cDNAs corresponding to Nox4, Nox2, p22^{phox}, and p67^{phox} were highlighted in the three chondrocyte cell lines (Fig. 2A). Data showed that Nox5 mRNA was also present in C-28/I2 and T/C-28a2, but not in the C-20/A4 cell line. None of the chondrocyte types expressed Nox1, Nox3, or p47^{phox} mRNA (Fig. 2A).

For the remaining experiments, the C-20/A4 cell line, which expresses only two Nox isoforms, was used. To assess the presence of Nox2 and p22^{phox} proteins, FACS experiments were carried out in both intact and permeabilized C-20A/4 chondrocytes with monoclonal antibodies directed against Nox2 (7D5) or p22^{phox} (44.1) (Fig. 2B) (5). There was no binding of either antibody 7D5 (Nox2) or 44.1 (p22^{phox}) on intact C-20/A4 cells, suggesting that the epitopes are not accessible. On the contrary, following permeabilization of chondrocytes with 0.01% (w/v) saponin, the mAb44.1 binding was significantly increased in comparison with results obtained with mAb7D5. The labeling on permeabilized but not on intact chondrocytes by mAb44.1 suggested a cytosolic accessible epitope for 44.1(p22^{phox}) in chondrocytes, as is reported in neutrophils (43). Finally, as shown with mAb7D5, there was a slight expression of gp91^{phox} (Nox2) in chondrocytes (Fig. 2B).

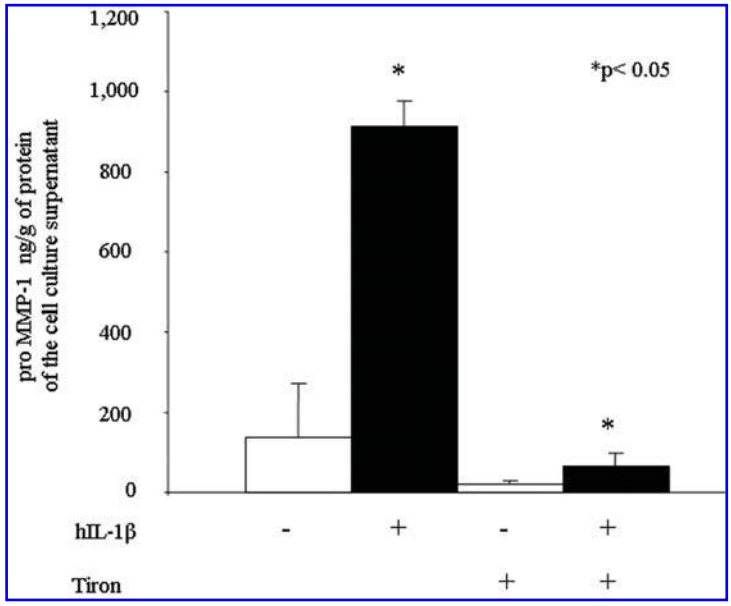

FIG. 1. Effect of cytokinic stress on MMP-1 expression in the C-20/A4 chondrocyte cell line. Monolayer-cultivated cells at 90% confluency were incubated with 500 pg/ml hIL-1β in the presence (or not) of 5 m*M* Tiron. After 23 h incubation, the supernatant was recovered for MMP-1 quantification by ELISA. Results are expressed as ng MMP-1/g of supernatant protein (measured by the Bradford technique). In addition, cell viability was verified by measurement of the LDH in the supernatant culture by an automated method (Hitachi automat). Values represent the mean ± S.E. of four experiments. *$p < 0.05$ versus nonstimulated cells; **$p < 0.05$ versus Tiron-free hIL-1β stimulated cells.

Overexpression of Nox4 isoforms (Nox4A and Nox4B) and Nox2

$p22^{phox}$ and Nox2 are present in the C-20/A4 chondrocyte cell line. To ascertain if the protein Nox4 was also present in these cells and to investigate functions of both Nox2 and Nox4, we generated a C-20/A4 chondrocyte cell line that provided a stable expression of Nox2 (Genbank No.NM000397), Nox4A (Nox4A-V5/His) (Genbank No.AF254621), or Nox4B (Nox4B-V5/His) (Genbank No. AY288918), in which the splicing of the exon 14 led to the lack of the first NAD(P)H binding site in the protein. Indeed, a previous study has shown that Nox4B was not able to produce ROS, and acted as a dominant-negative molecule for Nox4 (12).

Plasmid expression was checked in the C-20/A4 cell line by RT–PCR and results are shown in Fig. 3A. The data showed a slight mRNA expression of Nox2 and Nox4 in nontransfected C-20/A4 that was markedly increased in Nox2, Nox4A, and Nox4B overexpressing cell lines. PCR Nox4 mRNA expression in these cells was investigated in real time using primers that amplify a region commonly shared by Nox4A and Nox4B (Fig. 3B). This experiment revealed that Nox4 mRNA in C-20/A4 Nox4A-V5/His and C-20/A4 Nox4B-V5/His increased 22-fold and 5-fold, respectively. We confirmed that the amount of Nox4 mRNA remained unchanged in C-20/A4 cells expressing Nox2 or luciferase as a negative control (Fig. 3B).

Protein expression was assessed by FACS analysis in permeabilized cell lines. Nox2 expression is documented by two different types of monoclonal antibodies NL7 and 54.1 (Fig. 4A). The overexpressing cell line seems to have a weak, but significant, expression of Nox2 compared to baseline. Nox4A-V5His and Nox4B-V5His protein expression was checked by FACS analysis with two different antihistidine and anti-Nox4 polyclonal antibodies. The results show an increased expression of Nox4A and Nox4B in the two different cell lines (Fig. 4B). Absorption spectra confirmed the expression of Nox4A in C-20/A4 cell lines. Reduced minus oxidized differential spectra show the presence of a specific band at 426 nm in chondrocytes (Fig. 4B). The concentration of Nox4A increased significantly with overexpression (Fig. 3B).

Superoxide production

Since NAD(P)H oxidases are ROS-generating enzymes, it was of interest to investigate the effects of Nox2 and Nox4 variants on ROS generation. Because of its sensitivity, the chemiluminescence agent, luminol, was used to quantify hydrogen peroxide production in cells (for review, cf. Miller and Griendling, Ref. 29). Oxygen derivatives were quantified in experiments in which PMA and ionomycin stimulated C-20/A4 chondrocytes. Results illustrated in Fig. 5 showed a significant hydrogen peroxide synthesis in Nox4A-V5His transfected cells (14.87 RLU ± 0.44) compared with the control C-20/A4 (0.17 RLU ± 0.011) and with cells that express Nox4B (0.17 RLU ± 0.024). Moreover, no significant difference was observed after PMA and/or ionomycin stimulation, suggesting that neither Nox2 nor calcium is implicated in this H_2O_2 production. This reflects a constitutive generation of ROS mediated by Nox4 in C-20/A4 chondrocytes.

Intracellular levels of superoxide production were investigated in C-20/A4 cells with the DHE dye by fluorescence microscopy (Fig. 6). Nox4A overexpressing cells stimulated by 500 pg/ml hIL-1β produced significantly more superoxide (71,824 arbitrary units) than stimulated control C-20/A4 cells (7,993). Nox4A overexpressing cells that were not stimulated showed approximately a twofold reduction in fluorescence (35, 54). Moreover, the Nox4-mediated superoxide production was significantly reduced by the ROS scavenger *N*-acetylcysteine (NAC) (Fig. 6). Interestingly, Nox4B overexpressing cells produced less superoxide than control C-20/A4 cells after stimulation with hIL-1β. Indeed, in this case, the integral gray quantification was not possible as it appeared below the detection threshold of the software. These results confirm the dominant negative effect of Nox4B, as previously described (12, 17, 24).

MMP-1 production by hIL-1β stimulated C-20/A4 through Nox4

We and others have shown that hIL-1β increases MMP-1 production and excretion in C-20/A4 cell line (Fig. 1). To determine whether Nox4 or Nox2 have a role in this pathway, we

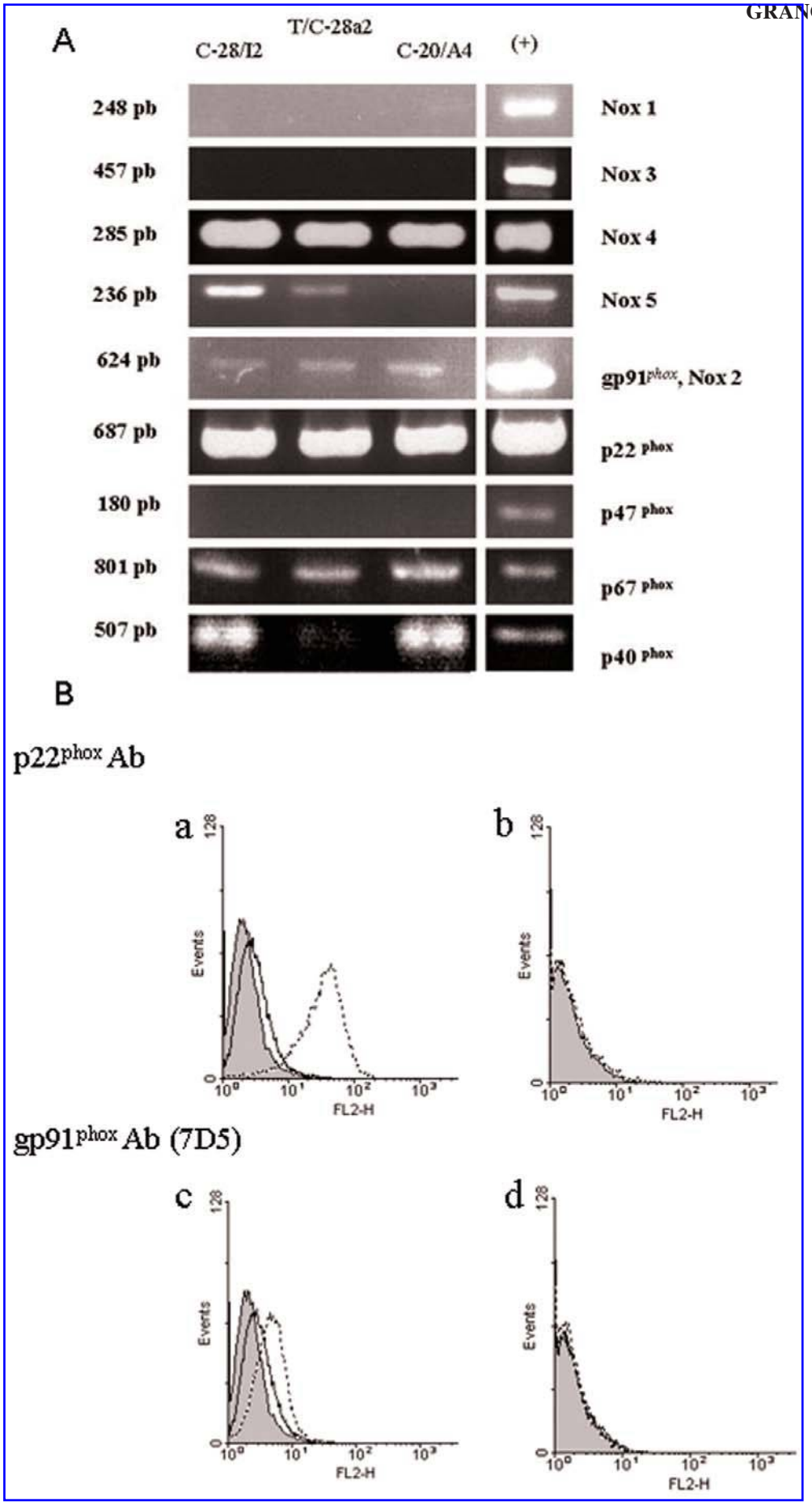
A
T/C-28a2
C-28/I2
C-20/A4
(+)
248 pb
Nox 1
457 pb
Nox 3
285 pb
Nox 4
236 pb
Nox 5
624 pb
gp91phox, Nox 2
687 pb
p22 phox
180 pb
p47 phox
801 pb
p67 phox
507 pb
p40 phox
B
p22phox Ab
a
b
Events
FL2-H
gp91phox Ab (7D5)
c
d

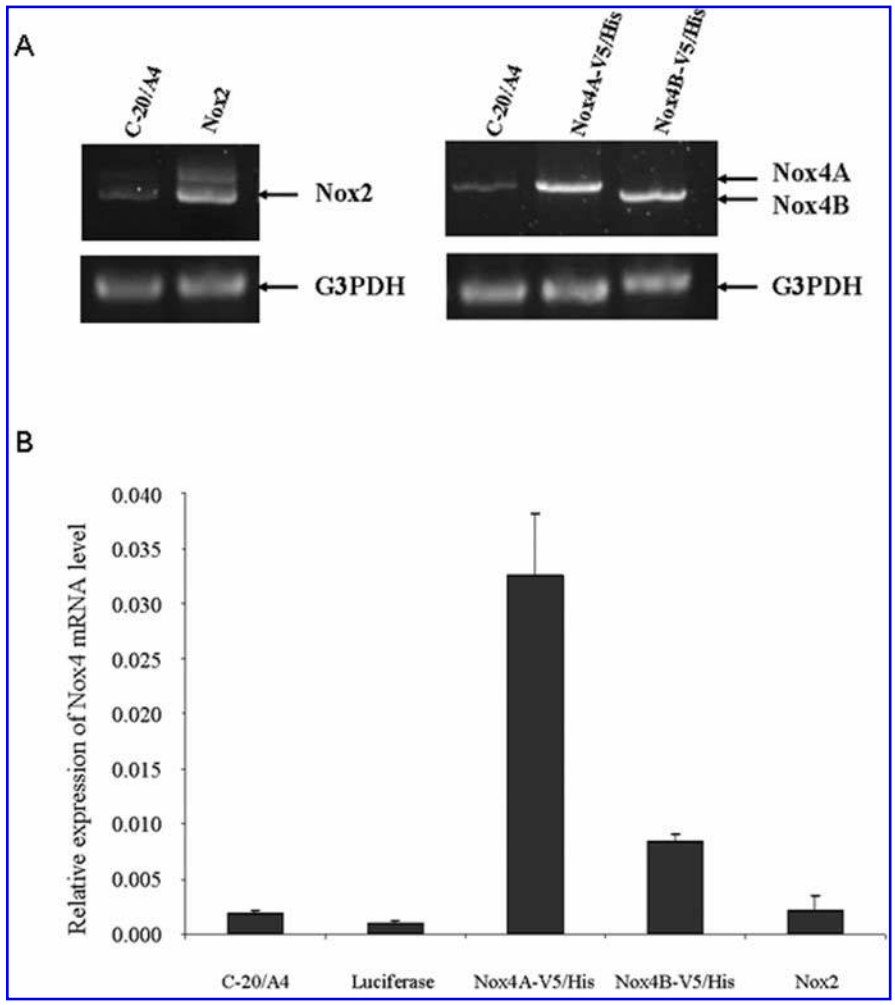

FIG. 3. Efficiency of plasmidic expression in transfected cells. (**A**) Total RNA was extracted from nontransfected C-20/A4 chondrocytes or Nox4A-V5/His, Nox4B-V5/His, or Nox2 transfected cells. PCRs for each plasmid were performed as previously described, using the primer sets F4'/R4' for Nox4 (characterizing both Nox4 isoforms), F2/R2 for Nox2, and commercial primers for G3PDH. (**B**) Nox4 mRNA expression by real-time RT–PCR. Total RNA was extracted from nontransfected C-20/A4 chondrocytes, Nox4A-V5/His, Nox4B-V5/His, luciferase, or Nox2 transfected cells. qRT–PCRs for each sample were performed as previously described, using the primer sets F4′′′/R4′′′ (characterizing both Nox4 isoforms). *Bars* indicate the relative expression of Nox4 versus G3PDH mRNA levels.

measured MMP-1 secretion under cytokinic stress in C-20/A4 cells that express both NAD(P)H oxidases. MMP-1 production by chondrocytes expressing Nox4A-V5His was increased by 3.6 (3,296.55 ng/g protein ± 1,789.11) compared with MMP-1 synthesis by control C-20/A4 cells (913.36 ng/g protein ± 64.54) (Fig. 7). However, there was no significant rise in MMP-1 secretion by cells expressing Nox2 or the Nox4B-V5His isoform. To demonstrate the specificity of MMP-1 production induced by Nox4, we used a truncated Nox4ΔFAD/NADPH protein described as a dominant-negative by Mahadev (17, 24). C-20/A4 cells expressing Nox4A-V5/His were transfected by an empty vector pCDNA 3.1 or by a pCDNA 3.1 Nox4ΔFAD/NADPH and exposed (or not) with hIL-1β (500 ng/ml) 48 h after transfection. The amount of MMP-1 was assessed in the cultured medium 23 h later. MMP-1 production by cells transfected by Nox4 dominant-negative (74 μg/g protein) was reduced by 66% compared to cells that had been transfected by the empty vector (215 μg/g protein) but not exposed to hIL-1β. The range of MMP-1 inhibition was the same between cells expressing Nox4AΔFAD/ NADPH (102 μg/g protein) and cells containing the empty vector (305 μg/g protein) incubated with hIL-1β. We verified that the construct gave raise to the functional protein Nox2 in PLB cells (data not shown).

DISCUSSION

In this study, we have described the presence of Nox4, one of the members of the NAD(P) H oxidase family, in chondrocytes. Moreover, we have demonstrated that Nox4 is directly

FIG. 2. mRNA and protein expression analysis of Nox and partners. (**A**) mRNA transcription analysis by RT–PCR. RNA was extracted from C-20/A4, T/C-28a2, and C-28/12 chondrocyte cell lines, and reverse transcripted to cDNA as described in the Materials and Methods section. Specific primer sets (*in parentheses*) were used to study the expression of Nox2 (F2/R2) $p22^{phox}$ (F6/R6), $p40^{phox}$ (F9/R9), $p47^{phox}$ (F8/R8), $p67^{phox}$ (F7/R7), Nox1 (F1/R1), Nox3 (F3/R3), Nox4 (F4/R4), and Nox5 (F5/R5). Positive controls (+) assess the efficiency of PCR experiments. They were performed on PLB8985, EBV-8 lymphocytes, or on plasmids that were encoded with Nox3 or Nox5. (B) Protein expression analysis by FACS, 5×10^5 C-20/A4 chondrocytes were fixed with 1% (w/v) paraformaldehyde and labeled with $p22^{phox}$ and $gp91^{phox}$ antibodies either immediately (*b, d*) or after saponin permeabilization (*a, c*), as described in the text. The antibodies used were: nonimmune immunoglobulin (*black solid line*; 5 μg/5×10^5 cells), anti-$gp91^{phox}$7D5, or anti-$p22^{phox}$ 44.1 (*black dotted line*, 5×10^5 cells), and phycoerythrine-conjugated secondary antibodies (dilution 1:200), no AB (*gray area*).

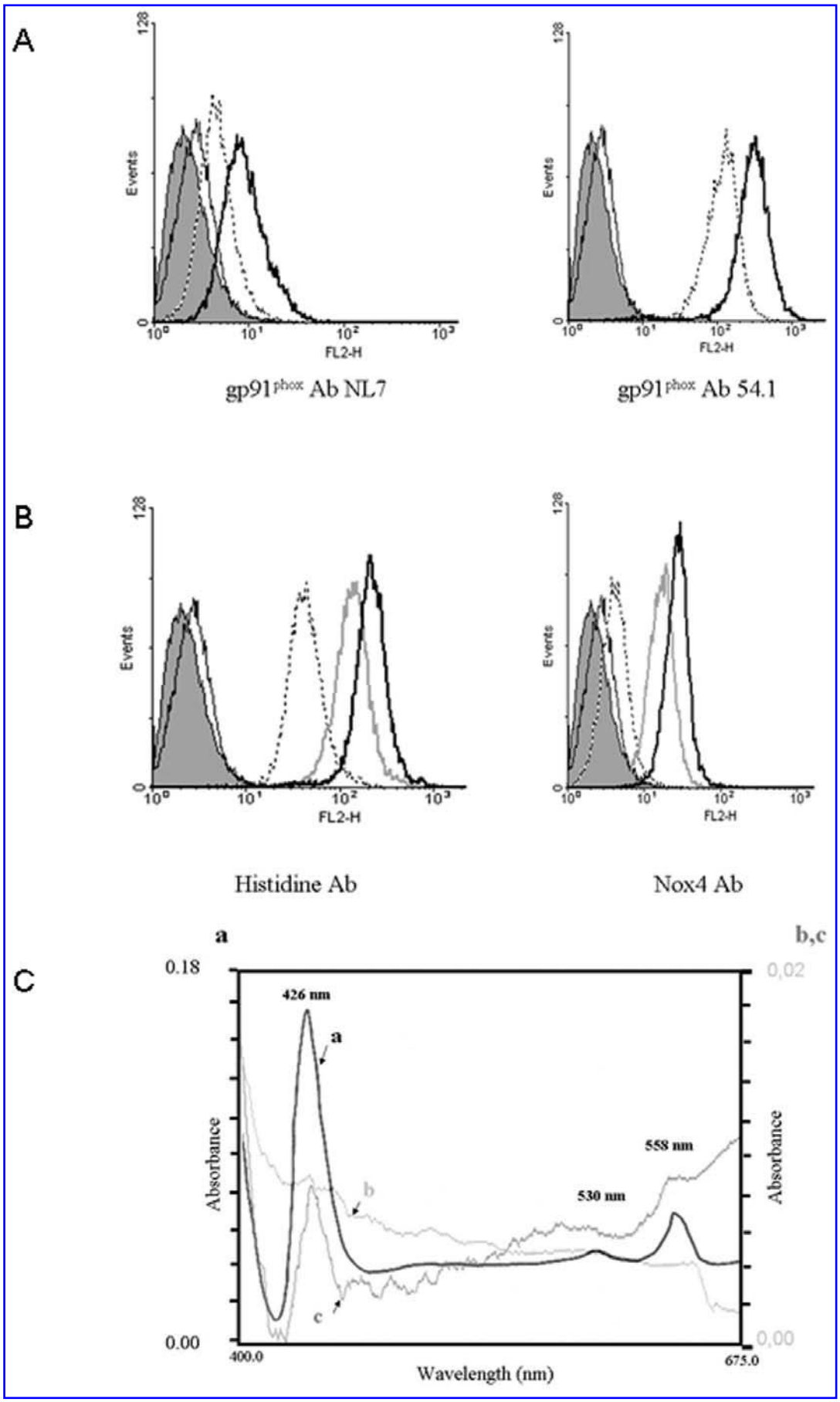
A
128
Events
0
10^0 10^1 10^2 10^3
FL2-H
gp91phox Ab NL7
gp91phox Ab 54.1
B
Histidine Ab
Nox4 Ab
C
a
b,c
0.18
0.00
0,02
0,00
426 nm
558 nm
530 nm
Absorbance
400.0
675.0
Wavelength (nm)

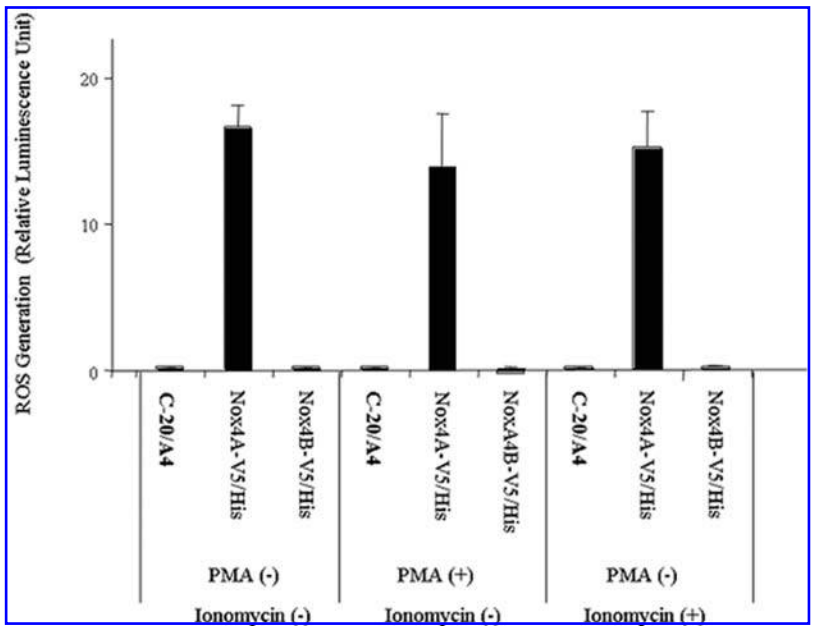

FIG. 5. Measurement of reactive oxygen species generation. ROS production was measured by chemiluminescence method from 5×10^5 intact C-20/A4 cells, Nox4A-V5/His, or Nox4B-V5/His transfected chondrocytes. Cells were stimulated or not with 80 ng/ml PMA and/or 2.5 μ*M* ionomycin. Results expressed the sum of all RLU measurements for 90 min for each condition. Values represent the mean ± S.E. of triplicate determinations obtained the same day.

involved in the expression of collagenase MMP-1, through the generation of ROS in response to the cytokinic stress, hIL-1β.

Human articular chondrocyte cell lines (C-20/A4, T/C-28a2, or C-28/I2) were developed to obtain reproducible cellular models, and used to study differentiated chondrocyte functions, and in particular, the cartilage-specific modulation induced by hIL-1β (7, 10, 36). All our experiments were carried out in the C-20/A4 cell line that expresses only Nox2 and Nox4 isoforms.

Oxidative stress was reported to increase the risk of osteoarthritis, but the precise mechanism remains unclear. It has been shown that it may lead to chondrocyte and cartilage senescence (50), and that cartilage degeneration can be mediated by locally produced matrix metalloproteinases (13). Finally, it was found that NAD(P)H oxidase-driven ROS production determines chondrocyte death and aggravates MMP-mediated cartilage destruction during osteoarthritis (46). There is now clear evidence that hIL-1β initiates inflammation (13, 18, 21), but it is necessary to investigate the specific pathway between the stimulus (hIL-1β) and the downstream inflammatory gene induction. The active phagocyte NADPH oxidase is a multiprotein complex in which the membrane-integrated protein $gp91^{phox}$ (Nox2) closely associates with $p22^{phox}$. Its activation requires assembly with $p47^{phox}$, $p67^{phox}$, and Rac.

$p47^{phox}$, which is a regulatory adaptor protein, is not present in the chondrocyte cell line C-20/A4: there is no possibility of oxidase activation, even if Nox2 is slightly expressed, as the complex does not assemble in the absence of $p47^{phox}$ (not shown) (47).

The close association of the Nox2 isoform with $p22^{phox}$ has recently been reported to be necessary for their enzymatic activity (1, 41). Our results demonstrate a significant coexpression of Nox4 and $p22^{phox}$, suggesting the presence of a functional Nox4 in chondrocytes. In all cell types where Nox4 has been identified, oxidase activity was shown to be constitutive. In this study, we have demonstrated that C-20/A4 chondrocyte oxidase activity of Nox4 was inducible. As expected, there was no significant increase in ROS production in Nox4B-V5/His overexpressing C-20/A4 cells. In fact, the truncated isoform Nox4 B has been reported to act as a dominant negative for Nox4 activity (12).

We have found that hIL-1β increases ROS production within 20 min after stimulation, which does not support a Nox neosynthesis. This suggests that Nox4 not only functions in a constitutive manner, but can also be activated by hIL-1β. The fact that the culture medium of hIL-1β stimulated C-20/A4 chondrocytes and the increase in MMP-1 argues in favor of a direct involvement of ROS as a secondary messenger leading to gene transcription of metalloproteinases. Further investigation into

FIG. 4. Nox2 and Nox4 expression analysis by FACS and cytochrome b spectroscopy. (**A**) $gp91^{phox}$ FACS analysis. 5×10^5 C-20/A4 WT or C-20/A4 Nox2 chondrocytes were fixed with 1% (w/v) paraformaldehyde and labeled with $gp91^{phox}$ (NL7 or 54.1) antibodies after saponin permeabilization, as described in the text. The following antibodies were used: nonimmune immunoglobulin (*black solid line*; 5 μg/5×10^5 cells), no Ab (*gray area*), and phycoerythrine-conjugated secondary antibodies (dilution 1:200). The C-20/A4 WT and C-20/A4 Nox2 were represented, respectively, by *black dotted line* and *black bold solid line.* (**B**) Nox4 FACS analysis. 5×10^5 C-20/A4WT, C-20/A4 Nox4A-V5/His, or C-20/A4 Nox 4B-V5/His chondrocytes were fixed with 1% (w/v) paraformaldehyde and labeled with antihistidine or anti-Nox4 antibodies after saponin permeabilization, as described in the text. The antibodies used were as in (**A**). The C-20/A4 WT were represented by a *black dotted line*; C-20/A4 Nox4A-V5/His and C-20/A4 Nox4B-V5/His, respectively, by *gray solid line* and *black bold solid line.* (**C**) The reduced minus oxidized difference spectra of C-20/A4 chrondrocyte cell line WT (*line b in gray*), transfected with Nox4 gene (*line c in gray*) were performed as described in the text, (positive conrol: cytochrome b558 purified from human neutrophils, absorbance at 426 nm using an ϵ 426 nm value of 106 $mM^{-1}.cm^{-1}$ or at 558 nm (ϵ 558 nm = 21.3 $mM^{-1}cm^{-1}$). The absorbance of the cytochrome b558 purified from human neutrophils (*line A*) was read at the *left side* of the figure, and the absorbance of the C-20/A4 chrondocyte cell line WT or transfected with Nox4 gene were read at the *right side* of the figure.

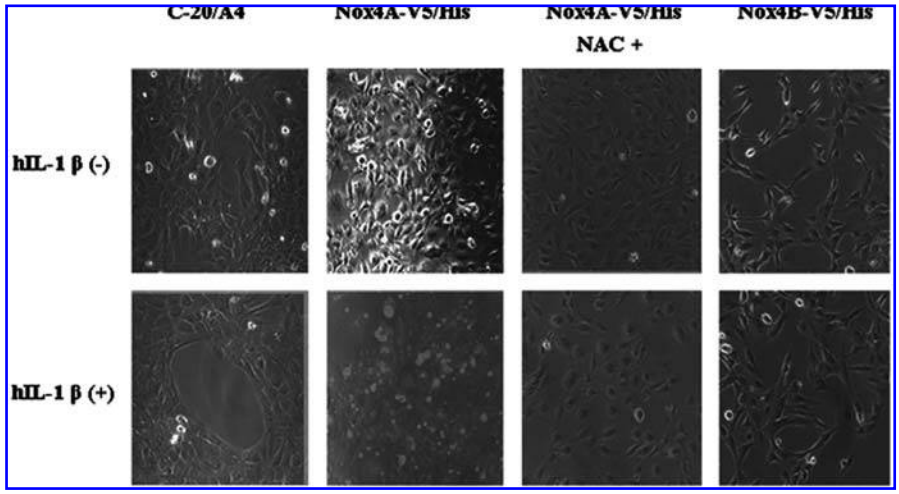

FIG. 6. Measurement of superoxide generation. Nontransfected chondrocytes C-20/A4, Nox4A-V5/His, or Nox4B-V5/His, or Nox2 transfected C-20/A4 were incubated with or without 500 pg/ml hIL-1β in the complete DMEM medium containing 5 μ*M* dihydroethidium (DHE) for 20 min in 6-well plates with or without 30 n*M* final NAC. Fluorometric measurements of the DHE oxidation in cell layers were carried out using a fluorescence microscope. Three replicates per treatment group were run for each experiment.

the specificity and modality of the signal transduction pathway is needed and this research opens a new area for therapeutic exploration.

Furthermore, we know that excessive and continuous cyclic mechanical stress and high magnitude cyclic tensile induce a production of IL-1β, MMP-1, and other MMPs, causing a quantitative imbalance between catabolic and anabolic pathways, ultimately resulting in cartilage degradation (8, 16).

What, then, is the role of ROS? Mechanical stress may increase a Nox4-mediated ROS production and activate matrix metalloproteinase expression: this question is currently being investigated.

ACKNOWLEDGMENTS

The authors acknowledge M. B. Goldring, A.L. Jesaitis, and M. J. Stasia for their generous gift of immortalized chondrocyte cell lines and monoclonal antibodies, and the Nox2 pEF-PGK neoplasmid, respectively. We thank S. Vergnaud, M. Guillot, and S. Papacatzis, for their helpful discussions, and G. Butt for his English revision. This work was supported by grants from the Ministère de l'enseignement supérieur de la recherche et technologie, MENRT, Paris; the Région Rhône-Alpes, programme Emergence; the Délégation Régionale à la Recherche Clinique – CHU Grenoble DRRC-CHU, Grenoble.

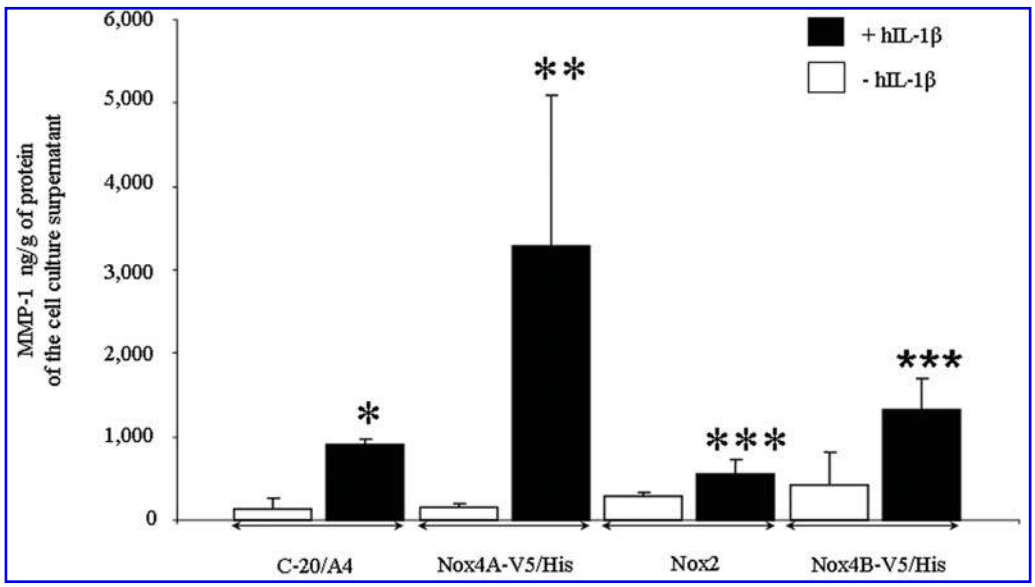

FIG. 7. Modulation of MMP-1 expression by Nox4 in C-20/A4 chrondrocytes, Nox4A-V5/His, Nox4B-V5/His, and Nox2 transfected cells. C-20/A4 cells were incubated for 23 h with or without 500 pg/ml hIL-1β. The culture medium was then recovered for MMP-1 quantification by ELISA. Results are expressed as ng MMP-1/g of supernatant protein (determined by the Bradford technique). In addition, cell viability was checked by measurement of the LDH in the supernatant culture. Values represent the mean ± S.E. of four determinations. *$p < 0.05$ versus nonstimulated cells; **$p < 0.05$ versus nontransfected hIL-1β stimulated cells; and ***$p < 0.05$ versus Nox4A-V5/His transfected hIL-1β stimulated cells.

ABBREVIATIONS

DHE, dihydroethidium; DMEM, Dulbecco's modified Eagle's medium; EBSS, Earle's balanced salts; FBS, fetal bovine serum; hIL-1β, human interleukin-1 beta; IgG1, immunoglobulin G1; LDH, lactate dehydrogenase; mAb, monoclonal antibody; MAPK, mitogen-activated protein kinase; NAC, *N*-acetylcysteine; OA, osteoarthitis; PBS, phosphate buffer saline; PMA, phorbol 12-myristate 13-acetate; MMP-1, metalloproteinase 1; ROS, reactive oxygen species; RT–PCR, reverse transcription– polymerase chain reaction.

REFERENCES

1. Ambasta RK, Kumar P, Griendling KK, Schmidt HH, Busse R, and Brandes RP. Direct interaction of the novel Nox proteins with $p22^{phox}$ is required for the formation of a functionally active NADPH oxidase. *J Biol Chem* 279: 45935–45941, 2004.
2. Benton HP and Tyler JA. Inhibition of cartilage proteoglycan synthesis by interleukin-I. *Biochem Biophys Res Commun* 154: 421–428, 1988.
3. Bionda C, Li XJ, Bruggen RV, Eppink M, Roos D, Morel F, and Stasia MJ. Functional analysis of two-amino acid substitutions in $gp91^{phox}$ in a patient with X-linked flavocytochrome b558-positive chronic granulomatous disease by means of transgenic PLB-985 cells. *Hum Genet* 115: 418–427, 2004.
4. Bradford MM. A rapid and sensitive method for the quantitation of microgram quantities of protein utilizing the principle of protein-dye binding. *Anal Biochem* 72: 248–254, 1976.
5. Burritt JB, DeLeo FR, McDonald CL, Prigge JR, Dinauer MC, Nakamura M, Nauseef WM, and Jesaitis AJ. Phage display epitope mapping of human neutrophil flavocytochrome b558. Identification of two juxtaposed extracellular domains. *J Biol Chem* 276: 2053–2061, 2001.
6. Burritt JB, Quinn MT, Jutila MA, Bond CW, and Jesaitis AJ. Topical mapping of neutrophil cytochrome *b* epitopes with phage-display libraries *J Biol Chem* 270: 16974–16980, 1995.
7. Finger F, Schörle C, Soder S, Zien A, Goldring MB, and Aigner T. Phenotypic characterization of human chondrocyte cell line C-20/A4: a comparison between monolayer and alginate suspension culture. *Cells Tissues Organs* 178: 65–77, 2004.
8. Fujisawa T, Hattori T, Takahashi K, Kuboki T, Yamashita A, and Takigawa M. Cyclic mechanical stress induces extracellular matrix degradation in cultured chondrocytes via gene expression of matrix metalloproteinases and interleukin-1. *J Biochem (Tokyo)* 125: 966–975, 1999.
9. Geiszt M, Kopp JB, Varnai P, and Leto TL. Identification of renox, an NAD(P)H oxidase in kidney. *Proc Natl Acad Sci USA* 97: 8010–8014, 2000.
10. Goldring MB, Birkhead JR, Suen LF, Yamin R, Mizuno S, Glowacki J, Arbiser JL, and Apperley JF. Interleukin-1 beta-modulated gene expression in immortalized human chondrocytes. *J Clin Invest* 94: 2307–2316, 1994.
11. Gorin Y, Block K, Hernandez J, Bhandari B, Wagner B, Barnes JL, and Abboud HE. Nox4 NAD(P)H oxidase mediates hypertrophy and fibronectin expression in the diabetic kidney. *J Biol Chem* 280:39616–39626, 2005.
12. Goyal P, Weissmann N, Rose F, Grimminger F, Schafers HJ, Seeger W, and Hanze J. Identification of novel Nox4 splice variants with impact on ROS levels in A549 cells. *Biochem Biophys Res Commun* 329: 32–39, 2005.
13. Gowen M, Wood DD, Ihrie EJ, Meats JE, and Russell RG. Stimulation by human interleukin-1 of cartilage breakdown and production of collagenase and proteoglycanase by human chondrocytes but not by human osteoblasts *in vitro*. *Biochim Biophys Acta* 797: 186–193, 1984.
14. Griendling KK. Novel NAD(P)H oxidases in the cardiovascular system. *Heart* 90: 491–493, 2004.
15. Hiran TS, Moulton PJ, and Hancock JT. Detection of superoxide and NAD(P)H oxidase in porcine articular chondrocytes. *Free Radic Biol Med* 23: 736–743, 1997.
16. Honda K, Ohno S, Tanimoto K, Ijuin C, Tanaka N, Doi T, Kato Y, and Tanne K. The effects of high magnitude cyclic tensile load on cartilage matrix metabolism in cultured chondrocytes. *Eur J Cell Biol* 79: 601–609, 2000.
17. Hu T, Ramachandrarao SP, Siva S, Valancius C, Zhu Y, Mahadev K, Toh I, Goldstein BJ, Woolkalis M, and Sharma K. Reactive oxygen species production via NAD(P)H oxidase mediates TGF-beta-induced cytoskeletal alterations in endothelial cells. *Am J Physiol Renal Physiol* 289: F816–F825, 2005.
18. Kheradmand F, Werner E, Tremble P, Symons M, and Werb Z. Role of Rac1 and oxygen radicals in collagenase-1 expression induced by cell shape change. *Science* 280: 898–902, 1998.
19. Krause KH. Tissue distribution and putative physiological function of NOX family NAD(P)H oxidases. *Jpn J Infect Dis* 57: S28–S29, 2004
20. Lambeth JD. NOX enzymes and the biology of reactive oxygen. *Nat Rev Immunol* 4: 181–189, 2004.
21. Le Maitre CL, Freemont AJ, and Hoyland JA. The role of interleukin-1 in the pathogenesis of human intervertebral disc degeneration. *Arthritis Res Ther* 7: R732–R745, 2005.
22. Liacini A, Sylvester J, Li WQ, and Zafarullah M. Inhibition of interleukin-1-stimulated MAP kinases, activating protein-1 (AP-1) and nuclear factor kappa B (NF-kappa B) transcription factors down-regulates matrix metalloproteinase gene expression in articular chondrocytes. *Matrix Biol* 21: 251–262, 2002.
23. Lo YY, Conquer JA, Grinstein S, and Cruz TF. Interleukin-1 beta induction of c-fos and collagenase expression in articular chondrocytes: involvement of reactive oxygen species. *Cell Biochem* 69: 19–29, 1998.
24. Mahadev K, Motoshima H, Wu X, Ruddy JM, Arnold RS, Cheng G, Lambeth JD, and Goldstein BJ. The NAD(P)H oxidase homolog Nox4 modulates insulin-stimulated generation of H2O2 and plays an integral role in insulin signal transduction. *Mol Cell Biol* 24: 1844–1854, 2004.
25. Martin G, Bogdanowicz P, Domagala F, Ficheux H, and Pujol JP. Rhein inhibits interleukin-1 beta-induced activation of MEK/ERK pathway and DNA binding of NF-kappa B and AP-1 in chondrocytes cultured in hypoxia: a potential mechanism for its disease-modifying effect in osteoarthritis. *Inflammation* 27: 233–246, 2003.
26. Mendes AF, Carvalho AP, Caramona MM, and Lopes MC. Diphenyleneiodonium inhibits NF-kappaB activation and iNOS expression induced by IL-1beta: involvement of reactive oxygen species. *Mediators Inflamm* 10: 209–215, 2001.

27. Mendes AF, Carvalho AP, Caramona MM, and Lopes MC. Differential roles of hydrogen peroxide and superoxide in mediating IL-1-induced NF-kappa B activation and iNOS expression in bovine articular chondrocytes. *J Cell Biochem* 88: 783–793, 2003.
28. Mengshol JA, Vincenti MP, Coon CI, Barchowsky A, and Brinckerhoff CE: Interleukin-1 induction of collagenase 3 (matrix metalloproteinase 13) gene expression in chondrocytes requires p38, c-Jun N-terminal kinase, and nuclear factor kappaB: differential regulation of collagenase 1 and collagenase 3. *Arthritis Rheum* 43: 801– 811, 2000.
29. Miller FJ and Griendling KK. Functional evaluation of non phagocytic NAD(P)H oxidases. *Methods Enzymol* 74: 220–233, 2002.
30. Moulton PJ, Hiran TS, Goldring MB, and Hancock JT. Detection of protein and mRNA of various components of the NADPH oxidase complex in an immortalized human chondrocyte line. *Br J Rheumatol* 36: 522–529, 1997.
31. Moulton PJ, Goldring MB, and Hancock JT. NADPH oxidase of chondrocytes contains an isoform of the gp91phox subunit. *Biochem J* 329: 449–451, 1998.
32. Nakamura M, Murakami M, Koga T, Tanaka Y, and Minakami S. Monoclonal antibody 7D5 raised to cytochrome b_{558} of human neutrophils: immunocytochemical detection of the antigen in peripheral phagocytes of normal subjects, patients with chronic granulomatous disease, and their carrier mothers. *Blood* 69: 1404–1408, 1987.
33. Paclet MH, Coleman AW, Vergnaud S, and Morel F. P67-phox-mediated NADPH oxidase assembly: imaging of cytochrome b_{558} liposomes by atomic force microscopy. *Biochemistry* 39: 9302–9310, 2000.
34. Paclet MH, Henderson LM, Campion Y, Morel F, and Dagher MC. Localization of Nox2 N- terminus using polyclonal antipeptide antibodies. *Biochem J* 382: 981–986, 2004.
35. Pedruzzi E, Guichard C, Ollivier V, Driss F, Fay M, Prunet C, Marie JC, Pouzet C, Samadi M, Eblin C, O'Dowd Y, Bens M, Vandewalle A, Gougerot–Pocidalo MA, Lizard G and Ogier–Denis E. NAD(P)H Oxidase Nox-4 mediates 7-ketocholesterol induced endoplasmic reticulum stress and apoptosis in human aortic smooth muscle cells. *Mol Cell Biol* 24:10703–10717, 2004.
36. Robbins JR, Thomas B, Tan L, Choy B, Arbiser JL, Berenbaum F, and Goldring MB. Immortalized human adult articular chondrocytes maintain cartilage-specific phenotype and responses to interleukin-1β. *Arthritis Rheum* 43: 2189–2201, 2000.
37. Sambrook J., Fritsch EF, and Maniatis T (Eds). *Molecular Cloning–A Laboratory Manual* (*2nd Ed*.) Cold Spring Harbor, NY: Cold Spring Harbor Laboratory Press, 1989.
38. Stasia MJ, Brion JP, Boutonnat J, and Morel F. Severe clinical forms of cytochrome b-negative chronic granulomatous disease (X91-) in 3 brothers with a point mutation in the promoter region of CYBB. *J Infect Dis* 188: 1593–1604, 2003.
39. Stasia MJ, Lardy B, Maturana A, Rousseau P, Martel C, Bordigoni P, Demaurex N, Morel F. Molecular and functional characterization of a new X-linked chronic granulomatous disease variant (X91+) case with a double missense mutation in the cytosolic gp91phox C-terminal tail. *Biochim Biophys Acta* 1586: 316–330, 2002.
40. Suliman HB, Ali M, and Piantadosi CA. Superoxide dismutase-3 promotes full expression of the EPO response to hypoxia. *Blood* 104: 43–50, 2004.
41. Sumimoto H, Miyano K, and Takeya R. Molecular composition and regulation of the Nox family NAD(P)H oxidases. *Biochem Biophys Res Commun. 338:* 677–686, 2005.
42. Tawara T, Shingu M, Nobunaga M, and Naono T. Effects of recombinant human IL-1 beta on production of prostaglandin E2, leukotriene B4, NAG, and superoxide by human synovial cells and chondrocytes. *Inflammation* 15: 145–157, 1991.
43. Taylor RM**,** Burritt JB, Baniulis D, Foubert TR, Lord CI, Dinauer MC, Parkos CA, and Jesaitis AJ. Site-specific inhibitors of NADPH oxidase activity and structural probes of flavocytochrome b: characterization of six monoclonal antibodies to the $p22^{phox}$ subunit. *J Immunol* 173: 7349–7357, 2004**.**
44. Trocme C, Gaudin P, Berthier S, Barro C, Zaoui P, and Morel F. Human B lymphocytes synthesize the 92-kDa gelatinase, matrix metalloproteinase-9. *J Biol Chem* 273: 20677–20684, 1998.
45. Van de Loo FA, Bennink MB, Arntz OJ, Smeets RL, Lubberts E, Joosten LA, van Lent PL, Coenen-de Roo CJ, Cuzzocrea S, Segal BH, Holland SM, and van den Berg WB. Deficiency of NADPH oxidase components p47phox and gp91phox caused granulomatous synovitis and increased connective tissue destruction in experimental arthritis models. *Am J Pathol* 163: 1525–1537, 2003.
46. Van Lent PL, Nabbe KC, Blom AB, Sloetjes A, Holthuysen AE, Kolls J, Van De Loo FA, Holland SM, and Van Den Berg WB. NADPH-oxidase-driven oxygen radical production determines chondrocyte death and partly regulates metalloproteinase-mediated cartilage matrix degradation during interferon-gamma-stimulated immune complex arthritis. *Arthritis Res Ther* 7: R885–895, 2005.
47. Vignais PV. The superoxide-generating NADPH oxidase: structural aspects and activation mechanism. *Cell Mol Life Sci* 59: 1428–1459, 2002.
48. Vincenti MP and Brinckerhoff CE. Early response genes induced in chondrocytes stimulated with the inflammatory cytokine interleukin-1beta. *Arthritis Res* 3: 381–388, 2001.
49. Yang S, Zhang Y, Ries W, and Key L. Expression of Nox4 in osteoclasts. *J Cell Biochem* 92: 238–248, 2004.
50. Yudoh K, Nguyen T, Nakamura H, Hongo–Masuko K, Kato T, and Nishioka K. Potential involvement of oxidative stress in cartilage senescence and development of osteoarthritis: oxidative stress induces chondrocyte telomere instability and downregulation of chondrocyte function. *Arthritis Res Ther* 7: R380–391, 2005.

Address reprint requests to:
Laurent Grange, M.D., Ph.D. student
GREPI EA 2938 UJF
Lab Enzymology/DBPC
Hospital A. Michallon
Grenoble 38043 Cedex 09, France

E-mail: LGrange@chu-grenoble.fr

Date of first submission to ARS Central, April 24, 2006; date of acceptance, April 26, 2006.

This article has been cited by:

1. Minh Vu Chuong Nguyen, Leilei Zhang, Stanislas Lhomme, Nicolas Mouz, Jean-Luc Lenormand, Bernard Lardy, Françoise Morel. 2012. Recombinant Nox4 cytosolic domain produced by a cell or cell-free base systems exhibits constitutive diaphorase activity. *Biochemical and Biophysical Research Communications* . [CrossRef]
2. Rasheed Ahmad, Judith Sylvester, Mushtaq Ahmad, Muhammad Zafarullah. 2011. Involvement of H-Ras and reactive oxygen species in proinflammatory cytokine-induced matrix metalloproteinase-13 expression in human articular chondrocytes. *Archives of Biochemistry and Biophysics* **507**:2, 350-355. [CrossRef]
3. Leilei Zhang, Minh Vu Chuong Nguyen, Bernard Lardy, Algirdas J. Jesaitis, Alexei Grichine, Francis Rousset, Monique Talbot, Marie-Hélène Paclet, GuanXiang Qian, Françoise Morel. 2011. New insight into the Nox4 subcellular localization in HEK293 cells: First monoclonal antibodies against Nox4. *Biochimie* **93**:3, 457-468. [CrossRef]
4. Jing-Li Tang, Wei-Ping Chen, Yan Xiong, Peng-Fei Hu, Li-Dong Wu. 2010. The anti-inflammatory effects of apocynin, inhibitor of NADPH oxidase, contrasting hyaluronic acid on articular cartilage during the development of osteoarthritis in a rabbit model. *Biomedicine & Pharmacotherapy* . [CrossRef]
5. Wendy Goodwin, Daniel McCabe, Ellen Sauter, Eric Reese, Morgan Walter, Joseph A. Buckwalter, James A. Martin. 2010. Rotenone prevents impact-induced chondrocyte death. *Journal of Orthopaedic Research* n/a-n/a. [CrossRef]
6. Hitesh Peshavariya , Fan Jiang , Caroline J. Taylor , Stavros Selemidis , Catherine W. T Chang , Gregory J. Dusting . 2009. Translation-Linked mRNA Destabilization Accompanying Serum-Induced Nox4 Expression in Human Endothelial Cells. *Antioxidants & Redox Signaling* **11**:10, 2399-2408. [Abstract] [Full Text HTML] [Full Text PDF] [Full Text PDF with Links] [Supplemental material]
7. Giuseppe Banfi, Eugenio L. Iorio, Massimiliano M. Corsi. 2008. Oxidative stress, free radicals and bone remodeling. *Clinical Chemistry and Laboratory Medicine* **46**:11, 1550-1555. [CrossRef]
8. C SEN, S ROY. 2008. Redox signals in wound healing. *Biochimica et Biophysica Acta (BBA) - General Subjects* **1780**:11, 1348-1361. [CrossRef]
9. F.L. Crane, H. Low. 2008. Reactive oxygen species generation at the plasma membrane for antibody control. *Autoimmunity Reviews* **7**:7, 518-522. [CrossRef]
10. Roman Ginnan, Benjamin J. Guikema, Katharine E. Halligan, Harold A. Singer, David Jourd'heuil. 2008. Regulation of smooth muscle by inducible nitric oxide synthase and NADPH oxidase in vascular proliferative diseases. *Free Radical Biology and Medicine* **44**:7, 1232-1245. [CrossRef]
11. Kathy K. Griendling . 2006. NADPH Oxidases: New Regulators of Old Functions. *Antioxidants & Redox Signaling* **8**:9-10, 1443-1445. [Citation] [Full Text PDF] [Full Text PDF with Links]